# Electromagnetic Field Distribution Modeling and Measuring of the 110 kV Substation

Dušan Medveď, Peter Žvanda
Department of Electrical Power Engineering
Mäsiarska 74
041 20 Košice, Slovak Republic
Dusan.Medved@tuke.sk , Peter.Zvanda@student.tuke.sk

*Abstract* — **This article deals with the solution of electromagnetic field distribution inside an electric 110 kV substation. The selected variables, which define the distribution of the electric and magnetic fields, in the respective place, were electric intensity *E* and magnetic induction *B*. Measurements were performed at three selected heights of 0.3 m; 1 m and 1.8 m above the ground, consisting of 168 measuring points along the selected part of the power-line. Subsequently, simulation was performed in ANSYS, where the distribution of electric and magnetic fields was solved. The measurement and simulation results were evaluated and compared with the action values set out in Decree 534/2007 Coll. (for residents) and 209/2016 Coll. (for employees).**

***Keywords: electric substation; electromagnetic field; electric intensity; magnetic induction***

## I. Introduction

This article analyzes and describes the distribution of the electromagnetic field (EMF) in a high voltage substation. The reason for addressing this issue was the fact that residents are increasingly appealing to a healthy environment and thus to avoiding harmful chemical or electromagnetic sources that cannot be registered by human sensors, but have an impact on the proper functioning of the organism itself. In Slovakia, the Decree of the Ministry of Health of the Slovak Republic no. 534/2007 Coll. (for residents) and government regulation 209/2016 Coll. (for employees), set exposure limit values and exposure action values for electromagnetic fields. These two documents are currently decisive for assessing whether a given source of electromagnetic radiation does not exceed the limit values, but since each living organism is different (in a professional language: it has different physical material properties), the real impact of an electromagnetic field on a living organism may be different.

For this reason, the present study and this paper were developed, which describes the measurement and computer simulation of electromagnetic field distribution in the 110 kV substation. The results of measurements and simulations were subsequently compared with the action values set out in Decree 534/2007 Coll.

## II. Measurement of Electromagnetic Field Distribution Around the Very High Voltage Substation

### A. Description of electrical substation

The measurement was carried out in a very high voltage substation in eastern Slovakia of a voltage level of 110 kV. The selected part of the electric array on which the measurement was made is shown in the following figure (Fig. 1). The measurement of the electromagnetic field was carried out separately for the electrical component and for the magnetic component. The selected array of the electric substation, where the measurement was carried out, contained 3-phase power-lines, consoles, supports, voltage instrument transformers, grounding, hence common equipment of electric array.

Figure 1. Illustration of the selected part of the power substation where the measurement was made

### B. List of measuring instruments

The FW Bell model 8030 Magnetometer Gaussmeter Teslameter was used to measure the electromagnetic field and its ***magnetic component*** along with an external 3-axis probe. Using this instrument, it was possible to measure the magnetic component of EMF in three axes ($x$, $y$, $z$). In addition to these three axes, the instrument measures the resulting vector value, i.e., the vector sum of the three axes. This makes it possible to measure the resulting value of the magnetic induction $\boldsymbol{B}$ that affects humans. In addition to the instrument, the 3-axis probe Z0A83-3208-10-T was used for the measurement. This probe, along with Gauss/Teslameter, allowed the magnetic induction to be measured from 0 T to 1 T. The measuring of EMF lasted for about 3 hours during constant weather, so thermal instability was not considered. Since it was necessary to move the probe in 3 axes, a fixed fastening structure of non-ferromagnetic material was provided. Accuracy of this device was 0,5 %.

The Gigahertz Solutions ME 3840B was used to measure the electromagnetic field and its ***electrical component***. Its frequency range is from 5 Hz to 100 kHz. The measuring range is limited to 0÷2000 V/m. This equipment is used to measure electromagnetic fields around the overhead power lines. This instrument contains an internal measuring probe (for both electric intensity and magnetic induction, but in this case it was used only for measuring the electric intensity). Accuracy of this device was 2 %.

## *C. Electromagnetic field measurement*

The electric substation consisted of a number of arrays, but one 110 kV array was chosen, where the load of this array was doubled compared to normal load, for measurement purposes. The marking of the measurement points is shown on the plan view of the substation array (Fig. 4).

The geometrical dimensions of the selected array were: length ($x$ axis) 15 400 mm and width ($y$ axis) 9 600 mm. An $x$-axis measurement step 2.2 m and $y$-axis 1.6 m were selected from the determined array dimensions. With this array size and the selected measurement steps, 56 measurement points were created. At each point, another three measurements were made at a height of 0.3 m; 1 m; 1.8 m. Together, 168 values of electric intensity ***E*** and 168 values of magnetic induction ***B*** were measured.

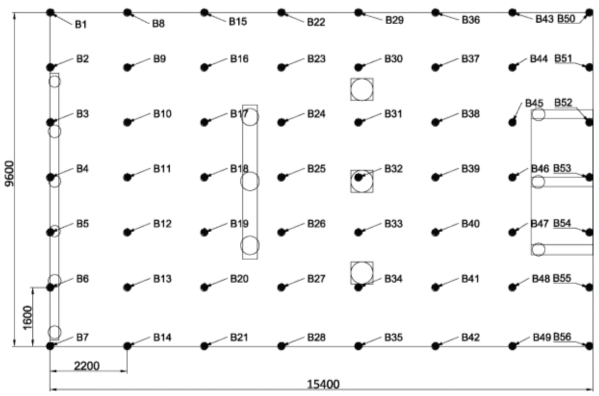


Figure 2. Plan view of the selected array in the electrical substation, indicating the measurement points

During measurement of ***E*** and ***B***, the ambient temperature was 19 °C and the humidity was 93 %. This humidity is relatively high and affected the measured results. The measurement of the electric field intensity was carried out in parallel with the measurement of the magnetic induction from 9:30 until 12:00. At the time of measurement, all three phases were loaded almost symmetrically. Mean effective current value in phases $L_1$, $L_2$, $L_3$ was $I_{L1} = 231.37$ A, $I_{L2} = 236.02$ A, $I_{L3} = 235.12$ A. The mean voltage at time of measurement was $U = 117{,}69$ kV. Later, the current and voltage values were used in the ANSYS simulation environment.

## *D. Measurement of magnetic induction **B***

Since number of measurement points is 168, only some selected outputs will be given in this paper in order to visualize and then assess the distribution of magnetic induction in selected locations of the array.

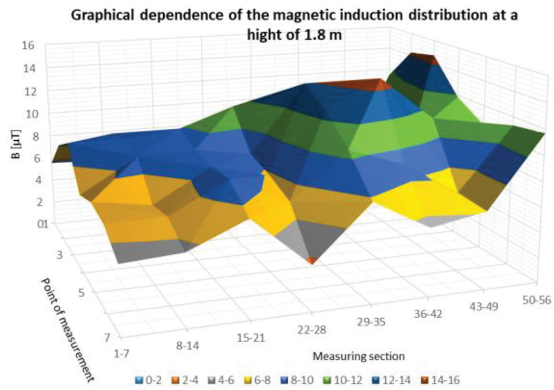


Figure 3. Graphical dependence of the magnetic induction distribution at height of 1.8 m from the ground

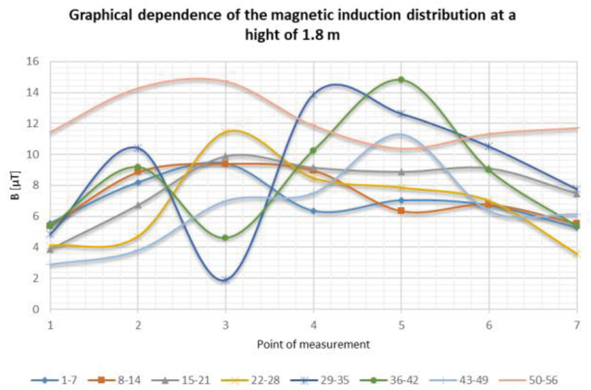


Figure 4. Graphical dependence of magnetic induction distribution in individual sections at a height of 1.8 m

A measurement at height of 1.8 m was made to detect the effect of magnetic induction on a human head. From the graphical dependence shown in Fig. 5, it is possible to see the large oscillations in all sections of the measurement. The largest oscillation was recorded in the measurement section 29-35, where the maximum value was at the fourth measurement point and was 13.89 μT (point B32, Fig. 4). Another oscillation was recorded in the measurement section 36-42 where the maximum value was at the fifth point of the measurement and was 14.81 μT (point B40). The overall increase in these values was in the section where the height of the cable was close above the ground due to the power switch that was located vertically (see Fig. 1). Therefore, when entering the power switch, the conductor's height above the ground was greater than that of the terminal where the height above the ground was less about 1.2 m. Therefore, the magnetic induction values also increased at all three stages. These values are comparatively as high as those measured in the last measurement section 50-56. In the measurement section 50-56, the magnetic induction along the whole section is the same as in the case of the magnetic induction measurement of 0.3 m and 1 m. The change occurs at the last point where the value of the magnetic induction no longer tends to rise, as it was at the previous heights, but stabilizes. The course of the magnetic induction curves in the individual sections can be observed in the Fig. 6. Each curve shows one section (cp. Fig. 4).

## *E. Measurement of electrical intensity **E***

Similar to the measurement of magnetic induction, as well as the measurement of electrical intensity ***E***, it was performed at 168 points. For the purpose of this paper, however, only essential results will be listed, suitable for visual assessment of the electric intensity distribution in selected area locations.

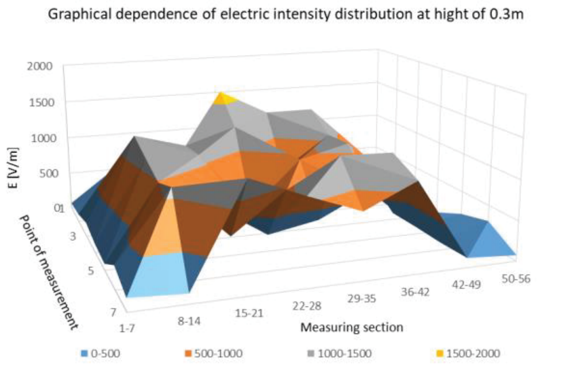


Figure 5. Graphical dependence of the electric intensity distribution at height of 0.3 m from the ground

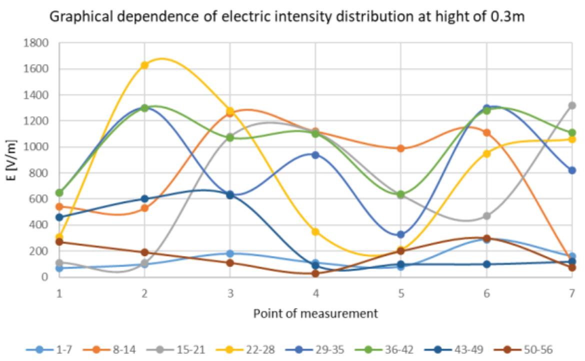


Figure 6. Graphical dependence of electric intensity distribution in individual sections at a height of 0.3 m

The graphical dependence in Fig. 8 shows the large fluctuations in all measuring sections. The smallest measured values of the electric field intensity were recorded in the first measurement section 1-7 and in the last measurement section 50-56. This is because in these sections, at the beginning and end of the array, is no large concentration of cables (phase conductors) of different constructions that would be the source of an electric field. The greatest oscillation was recorded in the measurement section 22-28, where the curve in this measurement section reached the greatest difference between the maximum and minimum values of the electric field intensity. The maximum value was at the second measurement point and was 1,630 V/m (point B23). This value is also the largest measured value at height of 0.3 m above the ground. In the other sections of the array, from the measurement section 8-14 to the measurement section 43-49, the measured values ranged from 400 V/m to 1300 V/m. In these sections, the instrumentation of the electric array is located. There are various consoles and high concentration of cables (phase conductors). The total electric intensity distribution throughout the array in this power substation is shown in Fig. 7.

*Note*: since the measuring instrument used did not allow the measurement of electrical intensity above 2000 V/m, the measurement at 1 m and 1.8 m was difficult and exceeded the stated measuring range of the instrument. Therefore, these values were verified and compared by simulation in ANSYS.

## III. Modeling of the Electromagnetic Field Distribution in ANSYS Environment

### *A. Design of geometry and meshing*

The simulation tool ANSYS Workbench was used to simulate the distribution of the electromagnetic field in which a 3D geometric model of the selected part of the array of 110 kV electric substation was created. In the first step, a detailed geometric model was created to provide more accurate EMF results. Due to the available computer technology (12-core processor, 96 GB RAM), where the ANSYS license is installed, it was found that it was not possible to obtain a meshed model after 2 weeks of operation. Therefore there was applied a gradual simplification of the geometric model, which was already applicable with given computer technology (for illustration: meshing of the model: 9 days (21 276 196 elements, mesh size 10 cm), magnetic induction calculation: 7 days, electric intensity calculation: 7 days).

### *B. Analysis of magnetic field distribution*

For the functionality of the whole model and its calculation it was necessary to define the material properties of the individual elements. All material properties are listed in Table I. This table shows the resistivity values needed to solve the electromagnetic field distribution (also for electric and magnetic fields). It also contains the relative permeability required for the magnetic field calculation. The resistivity value for electric and magnetic fields calculation was identical.

TABLE I. Electromagnetic Properties of Materials

| Material | Resistivity [Ω·m] | Relative permeability |
|---|---|---|
| Air | $2 \cdot 10^{14}$ | 1.00000037 |
| Aluminum | $8.21 \cdot 10^{-5}$ | 1.000022 |
| Concrete | $1 \cdot 10^{8}$ | 2 |
| Porcelain | $1 \cdot 10^{12}$ | 1 |
| Iron | $1.7 \cdot 10^{-7}$ | 100 |

The positioning of the probes in the model was the same (cf. Fig. 4) as in the case of real measurements, for the purpose of comparing the measured values with the simulated (at heights of 0.3 m, 1 m and 1.8 m above the ground).

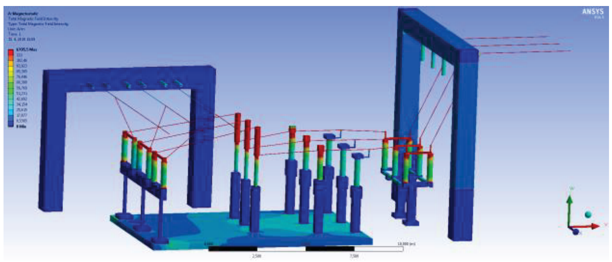

Figure 7. Magnetic field intensity ***H*** distribution in the measurement array (front view)

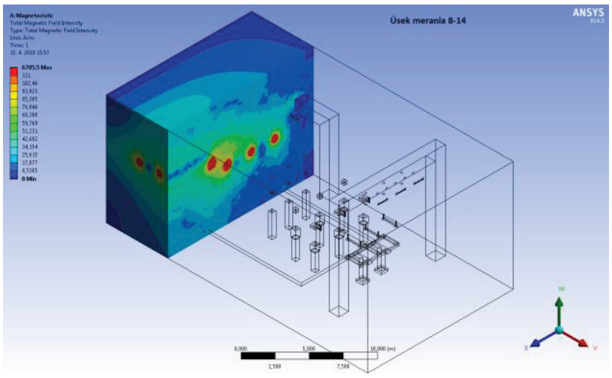


Figure 8. Visualisation of magnetic field intensity ***H*** distribution in selected measurement section 8-14

Similarly, it was possible to obtain a magnetic induction distribution ***B*** in the individual field locations (Fig. 11).

The magnetic induction distribution in the simulated array can be seen in Fig. 12 and Fig. 13. The magnitude of the magnetic induction distribution at height of 1.8 m is comparable to that of 1 m above the ground. As at a height of 1 m above the ground, as well as at this height of 1.8 m above the ground, the highest values of magnetic induction were recorded in the last measurement section 50-56. Values in this section were in the range of 40÷55 μT. In particular, the increase is seen at the beginning of the section at the point of measurement 2 and at the end of the section at the point of measurement 6. At these points there is a steel structure which serves to lead the conductors (and also power) out of the array. Therefore, in these locations, increased values arise due to the magnetic induction radiating from the phase conductors, (see Fig. 11). In the remaining sections, the curves of magnetic induction distribution are nearly the same. Values are in the range of 15÷45 μT.

It should be noted that the magnetic induction values at height of 0.3 m above the ground were considerably increased due to the grounding effect, which consisted of steel and concrete. The material properties of this grounding and geometric simplification (considered full ground, not latticed, and geometrically closer to the consoles for model simplifying and minimizing) had great impact to the simulation results.

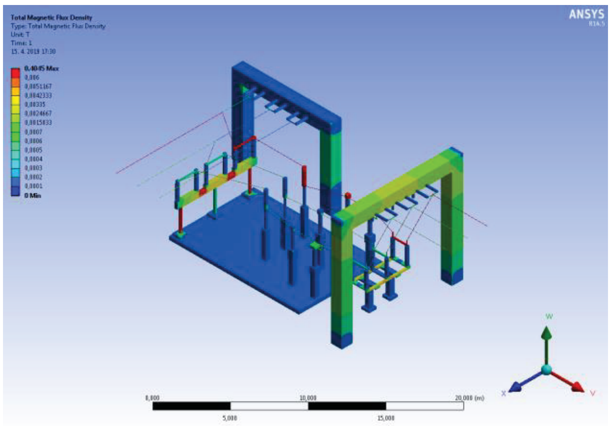


Figure 9. Magnetic induction distribution ***B*** in the measurement array (side view)

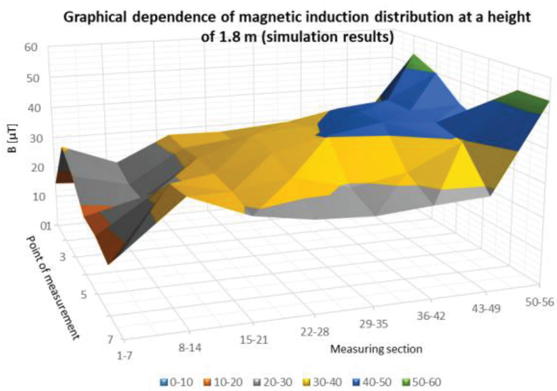


Figure 10. Graphical dependence of the magnetic induction distribution at height of 1.8 m from the ground

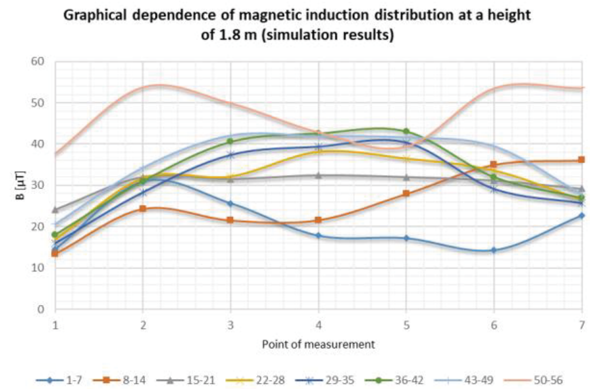


Figure 11. Graphical dependence of magnetic induction distribution in individual sections at a height of 1.8 m from the ground

## C. *Analysis of the electric field distribution*

For the purpose of simulation of the electric intensity distribution ***E***, the same mesh model was used as in the case of magnetic field. The properties that influence the electric field distribution are electric resistivity and relative permittivity.

The placement of the probes in the model was the same as in the case of real measurements (Fig. 4), for the purpose of comparing the measured values with the simulated (at height of 0.3 m, 1 m and 1.8 m). The results of the distribution of electrical intensity ***E*** at the selected locations and heights can be seen in the following graphs.

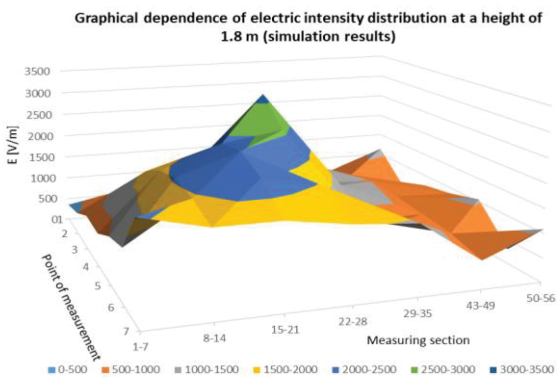


Figure 12. Graphical dependence of the electric intensity distribution at height of 1.8 m from the ground

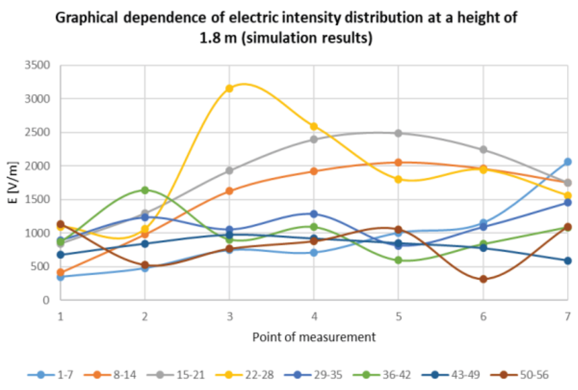


Figure 13. Graphical dependence of electric intensity distribution in individual sections at a height of 1.8 m above the ground

The graphical dependencies of electric intensity at height of 1.8 m above ground are in Fig. 14 and Fig. 15. It can be seen that in the most part of the array the electric intensity ***E*** is from 313.71 V/m to 1 282.5 V/m. However, there are also increased values in this height. Specifically, in the measurement range of 22-28, the value rapidly increases at the measurement point 3 to 3 152.4 V/m. Such an increase was due to a change in phase conductor height. The conductor (phase line) passes through the power switch, which is stored vertically. Therefore, the outgoing conductor from the power switch is positioned approximately 1.2 m lower than the input conductor. Therefore, such a decreasing of conductor height and increasing of measurement height caused an increase in the electric field intensity value. In the other two measurement sections, 8-14 and 15-21, a similar behavior of electric field intensity distribution is seen. These increases are caused by crossing conductors from the supplying power line and conductors in the array. Therefore, there are two sources that are the source of the electric field and therefore these values are also higher than the remaining values.

## IV. Comparison of Measurement and Simulation Results

Here it is worth mentioning that both the measurement results and the simulation results may have been influenced by several factors and thus have some accuracy. For example, the measurement probe of the instrument may be affected by the measurement, whether by EMF sources themselves or by the climatic conditions in which it was measured. Similarly, in simulations, results could be influenced, for example, by simplifying geometry, material constants of elements of electric substation, and so on. It follows from the above that the presented results have a certain accuracy (respectively measurement/simulation error) and serve only for illustrative comparison of individual characteristic values of the electromagnetic field.

### *A. Comparison of results for magnetic field*

TABLE II. Comparison of Maximum Magnetic Induction Value by Measurement/Simulation With National Legislation

| | Maximum measured / simulated value | Action value for employees (209/2016 Coll.) | Action value for residents (534/2007 Coll.) |
|---|---|---|---|
| *B* (μT) (0,3 m above ground) | 12.8 / 78.156 | 1 000 | 100 |
| *B* (μT) (1 m above ground) | 13 / 59.154 | 1 000 | 100 |
| *B* (μT) (1,8 m above ground) | 14.81 / 53.792 | 1 000 | 100 |

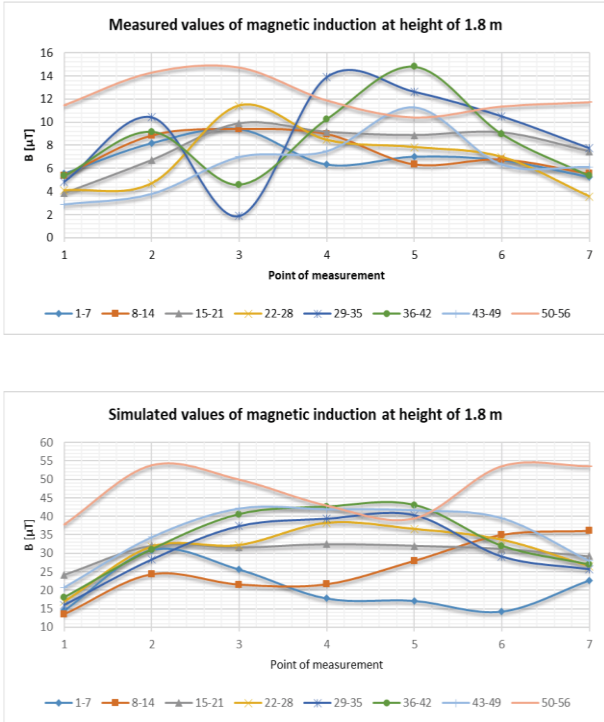


Figure 14. Measured and simulated values of magnetic induction at a height of 1.8 m above the ground

### *B. Comparison of results for electric field*

TABLE III. Comparison of Maximum Electric Intensity Value Obtained by Measurement/Simulation with National Legislation

| | Maximum measured / simulated value | Action value for employees (209/2016 Coll.) | Action value for residents (534/2007 Coll.) |
|---|---|---|---|
| *E* (V/m) (0,3 m above ground) | 1630 / 1 802.7 | 10 000 | 5 000 |
| *E* (V/m) (1 m above ground) | NA / 2 214.2 | 10 000 | 5 000 |
| *E* (V/m) (1,8 m above ground) | NA / 3 152.4 | 10 000 | 5 000 |

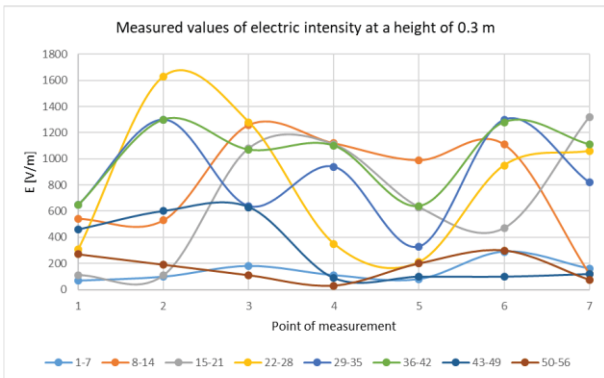

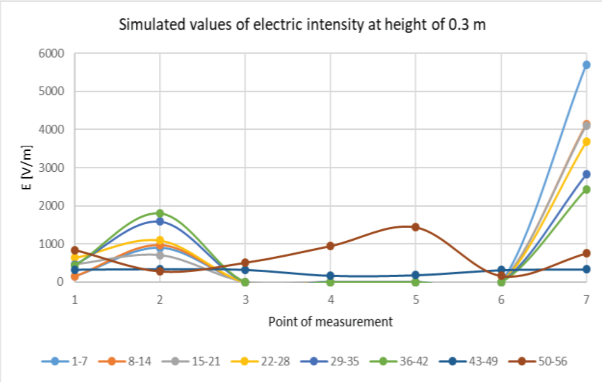


Figure 15. Values of electric intensity $E$ at a height of 0.3 m above the ground obtained by measurement and simulation

## V. Conclusion

The aim of this paper was to analyze and describe the distribution of the electromagnetic field inside the very high voltage power substation. The results of measurement and computer simulation of electromagnetic field distribution in 110 kV electrical substation are described in this paper. The results of measurements and simulations were compared with the action values set out in Decree of the Ministry of Health of the Slovak Republic no. 534/2007 Coll. (for residents) and government regulation 209/2016 Coll. (lower electric field intensity action values (RMS) were considered and compared in this case. For employees.), that set exposure limit values and exposure action values for electromagnetic fields. Other standards that are relevant for dealing with electromagnetic field are STN EN 50499; STN EN 50647; STN EN 62110.

When performing the measurement at the electrical substation, it was measured at three heights, in (0.3; 1; 1.8) m above the ground. The 168 measuring points were created along the whole array at the power substation. At a height of 0.3 m above the ground, the maximum electric field intensity of 1 630 V/m was measured. At subsequent heights, the measurement was limited due to an improperly selected measuring instrument that had a maximum measuring range of up to 2 000 V/m. The maximum measured magnetic induction value was 12.8 µT at a height of 0.3 m above the ground, 13 µT for a height of 1 m and 14.81 µT at a height of 1.8 m. In each measured height, neither the electric field intensity nor the magnetic induction it was not exceeded the action value in comparison with the action values found in Decree no. 534/2007 Coll. (for residents) and in regulation no. 209/2016 Coll. (for employees).

The simulation was realized in ANSYS environment. For the simulation, the measurement points were equally spaced as was the case with physical measurements. As one can see from the obtained results and the necessity of simplification of geometry and processing/calculation time, this software is not very useful for such a difficult geometry and there are necessary to accept lower accuracy for a long time calculation time. For this reason, we suggest to use different software for calculation of EMF in such a large object. The maximum simulated value of the magnetic induction was 78.156 µT at a height of 0.3 m above the ground, 59.154 µT at a height of 1 m and 53.792 µT at a height of 1.8 m above the ground. From this finding, it can be said that the action value of magnetic induction was not exceeded for both employees and ordinary citizens. For the electric field, the electric field intensity of 0.3 m above the ground was 1 802.7 V/m, for the height of 1 m it was 2 214.2 V/m and for the height of 1.8 m it was 3 152.4 V/m. Even the electric field has not exceeded the action values for employees and for ordinary people according to national legislation. It can be said that electric field modeling and its measured maximum values coincide with theoretical knowledge.

## Acknowledgement

This work was supported by the Ministry of Education, Science, Research and Sport of the SR and the Slovak Academy of Sciences under the contract No. VEGA 1/0372/18 and VEGA 1/0435/19.

## References

[1] D. Mayer, J. Polák, "*Metody řešení elektrických a magnetických polí*". SNTL/ALFA, Praha 1983.

[2] D. Rot, J. Jiřinec, J. Kožený, A. Podhrázký, J. Hájek, S. Jiřinec, „*Induction system for hardening of small parts*". In Proceedings of the 2018 19th International Scientific Conference on Electric Power Engineering (EPE). Piscataway: IEEE, 2018., p. 277-282. ISBN: 978-1-5386-4612-0, ISSN: 2376-5623.

[3] R. Cimbala, L. Kruželák, S. Bucko, J. Kurimský, M. Kosterec, *"Influence of Electromagnetic Interference on Time-Domain Spectroscopy of Magnetic Nanofluids"*, In: EPE 2016. Danvers: IEEE, 2016, p. 279 - 282. ISBN 978-1-5090-0907-7.

[4] M. Pavlík, *"Prediction of electricity price using RSI mechanism"*, In: Scientific Letters of Academic Society of M. Baludansky, Vol. 4, No. 6A (2016), p. 82-84. ISSN 1338-9432.

[5] J. Zbojovský, P. Liptai, M. Moravec, *"Modelling and calculating the shielding effectiveness of building materials"*, In: Technical sciences and technologies. Vol. 6, no. 4 (2016), p. 205-210. ISSN 2411-5363.

[6] M. Kanálik, M. Pavlík, M. Kolcun, *"The impact of multi-system overhead lines operation with different voltage levels to voltage unbalance"*, In: Elektroenergetika 2015. Košice: TU, 2015, p. 73-76. ISBN 978-80-553-2187-5.

[7] M. Kanálik, M. Kolcun, "*Computation of harmonic flows in three-phase systems*". In: Acta Electrotechnica et Informatica. Vol. 7, No. 3 (2007), p. 41-45. ISSN 1335-8243.

[8] J. Zbojovský, M. Pavlík, Z. Čonka, L. Kruželák, M. Kosterec, "*Influence of shielding paint on the combination of building materials for evaulation of shielding effectiveness*", In: EPE 2018. Brno: Un.ofTechn., p. 324-327. ISBN 978-1-5386-4611-3.

[9] J. Zbojovský, et al., "*Model of anechoic chamber for evaluating the shielding effectiveness of electromagnetic field*", Acta Techn. Corviniensis. Vol. 10, no. 3, pp. 159-161, ISSN 2067-3809.

[10] M. Tesařová, R. Vykuka, "*Impact of Distributed Generation on Power Flows Along Parallelly Operated MV Feeders*", Proceedings - 2018 IEEE International Conference on Environment and Electrical Engineering and 2018 IEEE Industrial and Commercial Power Systems Europe, EEEIC/I and CPS Europe 2018, DOI: 10.1109/EEEIC.2018.8493640.

[11] K. Nohac, M. Tesarova, L. Nohacova, J. Veleba, V. Majer, "*Utilization of Events Measured by WAMS-BIOZE-Detector for System Voltage Stability Evaluation*", IFAC-PapersOnLine, Volume 49, Issue 27, 2016, Pages 364-369, DOI: 10.1016/j.ifacol.2016.10.747.

[12] D. Kaprál, P. Braciník, M. Roch, M. Höger, "*Optimization of distribution network operation based on data from smart metering systems*", Electrical Engineering, Vol. 99, Issue 4, Springer, New York, USA, 2017, December, pp: 1417-1428, ISSN 0948-7921.

[13] Ž. Eleschová, A. Beláň, B. Cintula, B. Bendík, "*Smart grids analysis - View of the transmission systems voltage stability*", In EPE 2018. Brno: University of Technology, 2018, p. 37-42. ISBN 978-1-5386-4612-0.